

Enhanced two dimensional electron gas charge densities at III-III/I-V oxide heterostructure interfaces

Valentino R. Cooper*

Materials Science and Technology Division, Oak Ridge National Laboratory, Oak Ridge, TN 37831-6056

In this paper, density functional theory calculations are used to explore the electronic and atomic reconstruction at interfaces between III-III/I-V oxides. In particular, at these interfaces, two dimensional electron gases (2DEGs) with twice the interfacial charge densities of the prototypical $\text{LaTiO}_3/\text{SrTiO}_3$ heterostructure are observed. Furthermore, a significant decrease in the band effective masses of the conduction electrons is shown, suggesting that possible enhancements in electron mobilities may be achievable. These findings represent a framework for chemically modulating 2DEGs, thereby providing a platform through which the underlying physics of electron confinement can be explored with implications for modern microelectronic devices.

PACS numbers: 73.40.-c, 71.28.+d, 31.15.E-, 81.05.Zx

Emergent phenomena at ABO_3 oxide interfaces, e.g. two dimensional electron gases (2DEGs), [1] are paramount to understanding critical behavior arising from electron confinement; like metal-insulator transitions, [2] novel magnetic effects [3] and superconductivity, [4, 5] Recent theory and experiments have sought to identify the origin of 2DEGs at insulating oxide interfaces and surfaces in order to develop rules or concepts by which charge carrier densities and mobilities can be tuned. Growth under low O_2 partial pressure has been shown to have (vacancy mediated) enhancements in conductivities that extend deep into bulk regions, making these materials undesirable for examining interfacial physics. [6, 7] Conversely, annealing or growth under high O_2 pressure eliminates oxygen vacancies resulting in consequential increases in resistivities; giving rise to intrinsic 2DEG behavior. [6, 7] In oxide heterostructures such as $\text{LaAlO}_3/\text{SrTiO}_3$ and $\text{LaGaO}_3/\text{SrTiO}_3$ this is understood in terms of polarization discontinuities at interfaces, i.e. the “*the polar catastrophe*” mechanism. [6, 8–12] Physically, the divergence of the electrostatic potential at atomically abrupt interfaces between insulating layered, charge-ordered III-III and a non-polar II-IV (usually SrTiO_3) oxides is compensated for by charge accumulation (in this case an extra $1/2$ electron per interface unit cell) at the interface. Interestingly enough, in these heterostructures this only occurs at TiO_2 centered interfaces and requires relatively thick layers of LaAlO_3 or LaGaO_3 . [10, 13]

A chemically intuitive, δ -layer-doping, mechanism arises from the multivalent nature of transition metal cations, like Ti. For example, in $\text{LaTiO}_3/\text{SrTiO}_3$ superlattices, the local environment of Ti cations next to a “dopant”, LaO layer, splits the valence of Ti between two possible charge states (+4 for SrTiO_3 and +3 for LaTiO_3). Therefore, an equal mixture of Ti valence states (3+ or 4+) can be thought to reside at the interface giving an average valence of 3.5. [14–16] This has been confirmed through electron energy-loss spectroscopy (EELS) measurements [17] in which the dis-

tribution of Ti^{3+} cations away from the interface were found to be in good agreement with theoretical and experimental carrier density profiles. [6, 18–22] In a perfect system, the extra $1/2$ electron, relative to Ti in SrTiO_3 , defines the intrinsic limit of 2DEG carrier densities. [23] This electronic reconstruction is a hallmark of the observed two-dimensional conductivity and is accompanied by polar distortions [18, 24, 25] (atomic displacements of the cations away from the interface) which effectively screen the electrons near the interfaces. Furthermore, the most commonly studied 2DEGs derived from II-IV (e.g. $\text{Sr}^{2+}\text{Ti}^{4+}\text{O}_3$) oxides have interfacial carrier densities which are intrinsically limited to $0.5 e^-/\text{interface unit cell}$.

In this paper, density functional theory (DFT) calculations are used to investigate the charge rearrangement at interfaces between I-V/III-III perovskites. The goal is to apply the above insights to control the interfacial charge density by increasing the intrinsic limit of electrons at an oxide heterointerface. The guiding principle is that the incorporation of a multivalent cation at an interface, where its desired valence states are +3 and +5, should allow for an average valence of +4, thus increasing the limit of extra interfacial charge to $1 e^-/\text{interface unit cell}$. By examining heterostructures comprised of I-V/III-III oxides, it is confirmed that a total of 1 electron per interface unit cell now populates the conduction bands (twice that of a corresponding $\text{LaTiO}_3/\text{SrTiO}_3$ superlattice). Similar to previous observations of 2DEGs, these electrons are primarily confined to t_{2g} orbitals on B cations near LaO interfaces, decay quickly into the bulk and are accompanied by large polar ionic distortions. In addition, calculated decreases in electron band effective masses suggest that improved carrier mobilities may be achievable.

DFT calculations using the local density approximation with a Hubbard U (LDA+U) [26] and ultrasoft pseudopotentials [27] as implemented in the Quantum Espresso simulation package [28, 29] were performed to study 1 $\text{LaXO}_3/7 \text{KXO}_3$ superlattices, where $X=\text{Ta}$ and

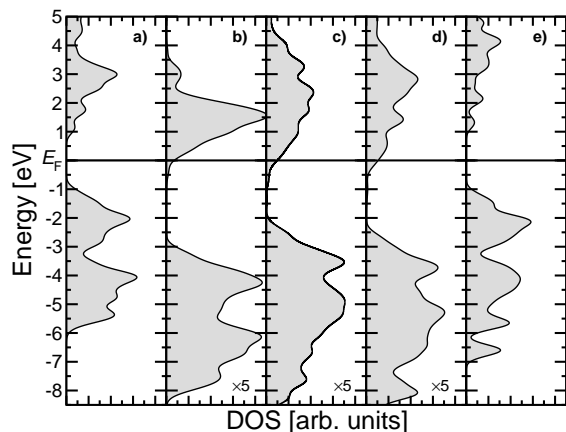


FIG. 1. DOS for (a) bulk SrTiO₃, (b) 1 LaTiO₃/7 SrTiO₃, (c) 1 LaNbO₃/7 KNbO₃ (d) 1 LaTaO₃/7 KTaO₃ and (e) bulk KTaO₃. All energies are relative to the Fermi level, E_F . (The scale for the heterostructures is $5\times$ that of the bulk structures.)

Nb. All superlattice calculations employed an 80 Ry cutoff and an $8\times 8\times 1$ k-point mesh. Comparisons were made with a prototypical 2DEG system, 1 LaTiO₃/7 SrTiO₃. In all calculations, the in-plane lattice constants were constrained to the theoretical value of the majority component (i.e. KXO_3 or SrTiO₃) and the out-of-plane, c , lattice vector was optimized within the P4mm space group with 1×1 in-plane periodicity. Simultaneously, all ionic coordinates were relaxed until all Hellman-Feynman forces were less than 8 meV/Å. The computed bulk KNbO₃, KTaO₃, and SrTiO₃ cubic lattice constants were 3.951 Å, 3.945 Å, and 3.855 Å, respectively. (Note: these values were obtained using standard LDA, i.e. without the inclusion of a Hubbard U). These are in typical LDA agreement with experimental values of 4.000 Å, 3.988 Å and 3.901 Å, respectively. For all heterostructure calculations, a Hubbard $U=5$ eV for B -cation d -states was found to be appropriate. Similar U values were used in previous studies of LaTiO₃/SrTiO₃.^[18, 25] Band effective masses were computed using quadratic fits of the partially occupied bands.

Figure 1 depicts the density of states (DOS) for bulk SrTiO₃, bulk KTaO₃, 1 LaTiO₃/7 SrTiO₃, 1 LaNbO₃/7 KNbO₃ and 1 LaTaO₃/7 KTaO₃ superlattices. Both SrTiO₃ and KTaO₃, using LDA (i.e. no Hubbard U) have relatively large band gaps of 1.7 and 1.8 eV, respectively. Although smaller than experiment, these are consistent with LDA's underestimation of oxide band gaps. In agreement with previous studies, 1 LaTiO₃/7 SrTiO₃ has occupied states just below the Fermi level, E_F , that sum to 1 electron (or rather 0.5 e^- /interface unit cell). The electronic band structure plot (Fig. 2a) indicates that they directly contribute to transport (i.e. cross the Fermi level). An analysis of the orbital projected DOS indicates that these states are derived mainly from Ti t_{2g}

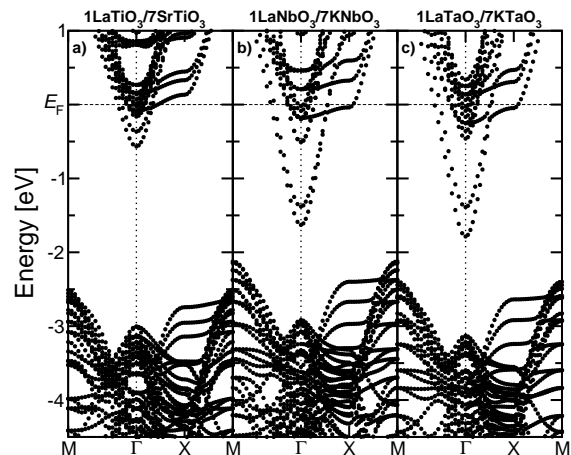


FIG. 2. Electronic band structure for (a) 1 LaTiO₃/7 SrTiO₃, (b) 1 LaNbO₃/7 KNbO₃ and (c) 1 LaTaO₃/7 KTaO₃ emphasizing the partially occupied states near the Fermi surface.

states, with the two lowest energy, light electron, bands coming almost entirely from d_{xy} orbitals on the interfacial Ti ions and the remaining occupied states being a mixture of t_{2g} states on all of the Ti cations. More importantly, in 1 LaNbO₃/7 KNbO₃ and 1 LaTaO₃/7 KTaO₃ these occupied electronic states sum up to exactly 2 electrons (i.e. 1 e^- / interface unit cell). An examination of the electronic band structure shows that they contribute to the Fermi surface (see Fig. 2b and c). Orbital projected DOS indicate that they are derived mainly from the B -cation d -states (Nb/Ta) with dominant electronic contributions arising from partially occupied d_{xy} orbitals of B -cations at the LaO interface. In all three heterostructures light electronic bands crossing E_F are parabolic around Γ and heavy bands extend along the Γ -X direction. This is a characteristic feature of 2DEGs and is consistent with recent angle-resolved photoemission spectroscopy (ARPES) results for 2DEGs at SrTiO₃ surfaces.^[20, 30]

Figure 3a displays the spatial distribution of the conduction electrons (i.e. arising from states between E_F and ~ -1.8 eV) as a function of distance away from the LaO layer. Similar to previous theoretical and experimental results for 2DEGs at heterointerfaces and the SrTiO₃ surface we find a build-up of charge of roughly 0.22 electrons on interfacial Ti cations in the 1 LaTiO₃/7 SrTiO₃ superlattice.^[6, 18–22] (Note: the total atom projected DOS adds up to 0.95 e^- and is scaled to unity in the plots.) This charge quickly decays to 0.06 electrons in the center of the slab, indicating a decay length of roughly 3-4 unit cells. On the other hand, we observe that the LaNbO₃/KNbO₃ and LaTaO₃/KTaO₃ heterostructures have a build-up of 0.52 and 0.60 e^- s on the interfacial Nb and Ta ions, respectively. (again the projected DOS only sums to 1.8 e^- s and is uniformly scaled to 2.0). Surprisingly, discernible differences in the

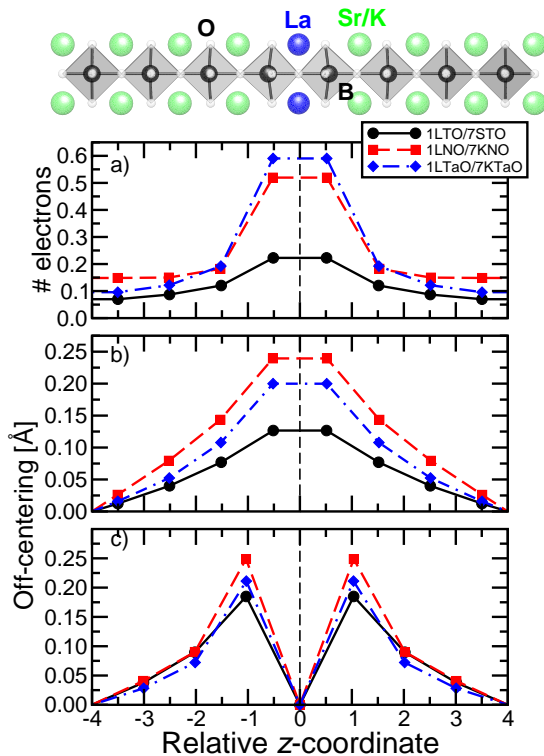


FIG. 3. (color online) [top] Representative 2-dimensional projection of a relaxed superlattices. (a) Charge distribution and (b) magnitude of B - and (c) A -cation off-centering as a function of relative z -coordinate for the superlattices studied. All distances are relative to LaO planes.

decay of charge away from the LaO interface are seen. In $\text{LaNbO}_3/\text{KNbO}_3$, there is still roughly $0.15 \text{ e}^-/\text{unit cell area}$ in the bulk region, whereas the charge density in $\text{LaTaO}_3/\text{KTaO}_3$ drops off much more sharply, falling to less than $0.1 \text{ e}^-/\text{unit cell area}$. This deviation may be linked to differences in dielectric constants. Theoretical calculations have demonstrated that a larger dielectric constant can result in a greater spread of electrons away from the interface.[31, 32] KTaO_3 and SrTiO_3 have very similar dielectric constants,[33, 34] while KNbO_3 has a much stronger dependence of dielectric constant on phase.[35] In fact, KNbO_3 can have a dielectric constants that is a few orders of magnitude greater than SrTiO_3 and KTaO_3 , making the observed behavior reasonable. Regardless, these results clearly indicate a significant enhancement in the concentration of electrons near the interface for III-III/II-IV heterostructure relative to the III-III/I-V system, with the lower dielectric constant materials being more conducive to confining electrons to the interface.

In accordance with the observed interfacial electronic reconstruction we find considerable polar distortions of the A - and B -cations away from the LaO layer. These off-center displacements gradually return to zero in the center of the $\text{SrTiO}_3/\text{KXO}_3$ layers. (See Fig. 3 [top] for

TABLE I. Structural parameters and relative effective masses for the heterostructures studied. a_o , c/a and m_e/m denote the cubic lattice parameter, c/a ratio and the relative effective masses of the two lowest energy partially occupied bands, respectively. Note: the curvature of the electronic structure around Γ is symmetric. i.e. the effective mass along the Γ -X and Γ -M directions are essentially equal and thus only one value is reported for each band.

System	a_o [Å]	c/a	m_e/m	
			1	2
1 $\text{LaTiO}_3/7 \text{ SrTiO}_3$	3.885	8.117	0.49	0.59
1 $\text{LaNbO}_3/7 \text{ KNbO}_3$	3.951	8.085	0.35	0.41
1 $\text{LaTaO}_3/7 \text{ KTaO}_3$	3.945	8.009	0.30	0.35

a representative 2 dimensional projection of the atomic structure of a 1/7 heterostructure). Similar to previous DFT results we find that the magnitude of SrTiO_3 off-centering is 0.18 Å and 0.13 Å for the A - and B -cations near the interface, respectively.[18, 25] Figure 3b and c show that the magnitudes of the B - and A -cation off-center displacements in the $\text{LaXO}_3/\text{KXO}_3$ structures are all appreciably larger than those in $\text{LaTiO}_3/\text{SrTiO}_3$. These larger polar distortions are consistent with the need for larger interfacial polarizations to adequately screen the interfacial charges. Unexpectedly, the $\text{LaTaO}_3/\text{KTaO}_3$ superlattice while having the larger interfacial charge exhibits smaller polar distortions than $\text{LaNbO}_3/\text{KNbO}_3$. Although the difference in the computed interfacial charge may be a consequence of scaling of the charge densities, it may also be a direct indicator of the magnitude of charge screening in these two materials arising from the differences in their respective dielectric constants - with the lower dielectric constant material being more strongly screened. A second explanation is that KNbO_3 , unlike KTaO_3 , has a polar ground state which may be more favorable to inducing polar distortions. In which case, the polar nature of the KNbO_3 structure may be more advantageous as recent studies have proposed the use of an electric field as a switch for controlling interface conductivity.[24, 36]

Finally, Table I lists the relative band effective masses, m_e/m , of the two lowest energy partially occupied bands (see Fig. 2). Remarkably, the computed m_e/m values for SrTiO_3 , are in excellent agreement with ARPES measurements performed for SrTiO_3 surface 2DEGs ($0.5 - 0.6 m_e/m$).[30] While the origin of the 2DEGs at SrTiO_3 surfaces is almost certainly due to a different mechanism than the δ -doped structures, this result is suggestive of characteristic electronic structure features. It should be pointed out that La doped SrTiO_3 has considerably higher effective mass ($m_e/m > 1$) and that the band effective masses predicted here neglects correlation effects. Moreover, the 1 $\text{LaXO}_3/7 \text{ KXO}_3$ structures were found to have significant decreases in m_e for these bands

(which dominate the electron density at the interfaces), implying possible increases in carrier mobilities in the III-III/I-V superlattices. Of course, semiconductor physics tells us that increases in charge densities (as observed in the 1 LaXO₃/7 KXO₃ based heterostructures) are often accompanied by decreases in carrier mobilities. Typically increased carrier densities arise from increases in dopant concentrations, which act as scattering centers thereby reducing the mean free path of the carriers. In the above materials the LaO layers could be considered dopants (i.e. δ -doped layers). Since the concentration of La remains constant at the interface there may be little change in the scattering lifetimes, τ . Hence, deviations in electron mobilities, μ_e , may be more affected by changes in m_e (where $\mu_e = e\tau/m_e$). Furthermore, recent dynamical-mean-field calculations of oxide heterostructure 2DEGs suggest that correlation effects are least affected by dopant concentrations and that the band effective masses have the most deviations.[37]

In summary, using first principles methods, it is demonstrated that superlattices comprising I-V (K¹⁺[Nb/Ta]⁵⁺O₃) and III-III (La³⁺[Nb/Ta]³⁺O₃) perovskites have twice the interfacial charge densities of III-III/II-IV (SrTiO₃/LaTiO₃) superlattices. Here, the flexibility of multivalent cations, like Nb and Ta, leads to an intrinsic limit of 1 e⁻ per interface unit cell, twice the limit of previously studied III-III/II-IV and I-V/III-III [24, 38] superlattices. Also, changes in electron effective masses (with no change in dopant levels) imply that further enhancements in mobilities may be achievable. As such, this research highlights a viable path for enhancing the properties of 2DEGs. In addition, deviations in polar distortions and charge redistribution emphasize the need for a better understanding of the relationship between dielectric constant and electronic and atomic reconstructions. In agreement with other theoretical models,[31, 32] these results suggest that lower dielectric constant materials (e.g. KTaO₃) should be more ideal for realizing truly two-dimensional electronic gases. Alternatively, polar oxides like KNbO₃ may be more suitable for applications where it is necessary to switch the charge carrier concentrations. Naturally, synthetic limitations related to effectively reducing ions like Ta⁵⁺ to Ta³⁺ may exist. A feasible route may be to substitute interfacial Ta cations with a cation, like V, that is more easily reduced. Ultimately, these results present a chemically intuitive framework (in the absence of factors such as O vacancies) through which intrinsic carrier concentrations, and perhaps even carrier mobilities, of oxide heterostructure 2DEGs can be tuned and may be useful in device engineering [39] and in controlling quantum phenomena due to electron confinement.

V.R.C. would like to acknowledge helpful discussions with C. Bridges, C. Cantoni, H. N. Lee, S. Okamoto, D. Parker, W. Siemons and D. Xiao. This work was supported by the Materials Sciences and Engineering Divi-

sion, Office of Basic Energy Sciences, U.S. Department of Energy. This research used resources of the National Energy Research Scientific Computing Center, supported by the Office of Science, U.S. Department of Energy under Contract No. DEAC02-05CH11231.

* coopervr@ornl.gov

- [1] A. Ohtomo, D. A. Muller, J. L. Grazul, and H. Y. Hwang, *Nature* **419**, 378 (2002).
- [2] S. Thiel, G. Hammerl, A. Schmehl, C. W. Schneider, and J. Mannhart, *Science* **313**, 1942 (2006).
- [3] A. Brinkman, M. Huijben, M. van Zalk, J. Huijben, U. Zeitler, J. C. Maan, W. G. van der Wiel, G. Rijnders, D. H. A. Blank, and H. Hilgkamp, *Nat. Mater.* **6**, 493 (2007).
- [4] K. v. Klitzing, G. Dorda, and M. Pepper, *Phys. Rev. Lett.* **45**, 494 (1980).
- [5] T. Ando, A. B. Fowler, and F. Stern, *Rev. Mod. Phys.* **54**, 437 (1982).
- [6] W. Siemons, G. Koster, H. Yamamoto, W. A. Harrison, G. Lucovsky, T. H. Geballe, D. H. A. Blank, and M. R. Beasley, *Phys. Rev. Lett.* **98**, 196802 (2007).
- [7] A. Kalabukhov, R. Gunnarsson, J. Börjesson, E. Olsson, T. Claeson, and D. Winkler, *Phys. Rev. B* **75**, 121404 (2007).
- [8] A. Ohtomo and H. Y. Hwang, *Nature* **427**, 423 (2004).
- [9] N. Nakagawa, H. Y. Hwang, and D. A. Muller, *Nat. Mater.* **5**, 204 (2006).
- [10] R. Pentcheva and W. E. Pickett, *Phys. Rev. Lett.* **102**, 107602 (2009).
- [11] N. C. Bristowe, E. Artacho, and P. B. Littlewood, *Phys. Rev. B* **80**, 045425 (2009).
- [12] M. Stengel and D. Vanderbilt, *Phys. Rev. B* **80**, 241103 (2009).
- [13] P. Perna, D. Maccariello, M. Radovic, U. S. di Uccio, I. Pallecchi, M. Codda, D. Marr, C. Cantoni, J. Gazquez, M. Varela, S. J. Pennycook, and F. M. Granozio, *Appl. Phys. Lett.* **97**, 152111 (2010).
- [14] G. A. Baraff, J. A. Appelbaum, and D. R. Hamann, *Phys. Rev. Lett.* **38**, 237 (1977).
- [15] W. A. Harrison, E. A. Kraut, J. R. Waldrop, and R. W. Grant, *Phys. Rev. B* **18**, 4402 (1978).
- [16] H. Chen, A. M. Kolpak, and S. Ismail-Beigi, *Adv. Mater.* **22**, 2881 (2010).
- [17] H. W. Jang, D. A. Felker, C. W. Bark, Y. Wang, M. K. Niranjan, C. T. Nelson, Y. Zhang, D. Su, C. M. Folkman, S. H. Baek, S. Lee, K. Janicka, Y. Zhu, X. Q. Pan, D. D. Fong, E. Y. Tsymbal, M. S. Rzchowski, and C. B. Eom, *Science* **331**, 886 (2011).
- [18] S. Okamoto, A. J. Millis, and N. A. Spaldin, *Phys. Rev. Lett.* **97**, 056802 (2006).
- [19] S. Okamoto and A. J. Millis, *Nature* **428**, 630 (2004).
- [20] A. F. Santander-Syro, O. Copie, T. Kondo, F. Fortuna, S. Pailhes, R. Weht, X. G. Qiu, F. Bertran, A. Nicolaou, A. Taleb-Ibrahimi, P. Le Fevre, G. Herranz, M. Bibes, N. Reyren, Y. Apertet, P. Lecoer, A. Barthelemy, and M. J. Rozenberg, *Nature* **469**, 189 (2011).
- [21] C. Cantoni, J. Gazquez, F. M. Granozio, M. P. Oxley, M. Varela, A. R. Lupini, S. J. Pennycook, C. Aruta, U. S. di Uccio, P. Perna, and D. Maccariello, (2011), (Unpub-

- lished).
- [22] M. Takizawa, S. Tsuda, T. Susaki, H. Y. Hwang, and A. Fujimori, arXiv:1106.3619v1.
- [23] J. S. Kim, S. S. A. Seo, M. F. Chisholm, R. K. Kremer, H.-U. Habermeier, B. Keimer, and H. N. Lee, Phys. Rev. B **82**, 201407(R) (2010).
- [24] Y. Wang, M. K. Niranjan, S. S. Jaswal, and E. Y. Tsymbal, Phys. Rev. B **80**, 165130 (2009).
- [25] D. R. Hamann, D. A. Muller, and H. Y. Hwang, Phys. Rev. B **73**, 195403 (2006).
- [26] V. I. Anisimov, J. Zaanen, and O. K. Andersen, Phys. Rev. B **44**, 943 (1991).
- [27] D. Vanderbilt, Phys. Rev. B **41**, 7892(R) (1990).
- [28] M. Cococcioni and S. de Gironcoli, Phys. Rev. B **71**, 035105 (2005).
- [29] P. Giannozzi, *et al.*, J. Phys.: Cond. Matt. **21**, 395502 (2009).
- [30] W. Meevasana, P. D. C. King, R. H. He, S. K. Mo, M. Hashimoto, A. Tamai, P. Songsiriritthigul, F. Baumberger, and Z. X. Shen, Nat. Mater. **10**, 114 (2011).
- [31] S. Okamoto and A. J. Millis, Phys. Rev. B **70**, 075101 (2004).
- [32] S. S. Kancharla and E. Dagotto, Phys. Rev. B **74**, 195427 (2006).
- [33] M. D. Agrawal and K. V. Rao, J. Phys. C: Solid State Phys. **3**, 1120 (1970).
- [34] G. Rupprecht and R. O. Bell, Phys. Rev. **135**, A748 (1964).
- [35] G. Shirane, H. Danner, A. Pavlovic, and R. Pepinsky, Phys. Rev. **93**, 672 (1954).
- [36] A. D. Caviglia, S. Gariglio, N. Reyren, D. Jaccard, T. Schneider, M. Gabay, S. Thiel, G. Hammerl, J. Mannhart, and J. M. Triscone, Nature **456**, 624 (2008).
- [37] S. Okamoto, Phys. Rev. B (Rapid) **84** (2011).
- [38] E. D. Murray and D. Vanderbilt, Phys. Rev. B **79**, 100102 (2009).
- [39] J. Mannhart and D. G. Schlom, Science **327**, 1607 (2010).